NANOSTRUCTURES

PACS numbers: 81.16.Mk; 78.67.–n; 42.65.An
DOI: 10.1070/QE2014v044n11ABEH015308

Investigation of the nonlocal nonlinear optical response of copper nanostructured thin films prepared by pulsed laser deposition

B. Farmanfarmaei, M.R. RashidianVaziri, F. Hajiesmaeilbaigi

Abstract. **Nanostructured copper thin films have been prepared using the pulsed laser deposition method. Optical absorption spectra of these films exhibit plasmonic absorption peaks around 619 nm, which suggests the formation of copper nanoparticles on their surfaces. Scanning electron micrographs of the films confirm the nanoparticle formation on the films surfaces. After laser beam passing through the thin films, the observed diffraction rings on a far-field screen have been recorded. Despite the smallness of the maximal axial phase shifts of the films, which have been obtained using the nonlocal *z*-scan theory, a series of low-intensity rings can be observed on the far field screen for some specific positions of the thin films from the focal point. It is shown that the best approach to determining the sign and magnitude of the nonlinear refractive index of thin samples is the application of the conventional close-aperture *z*-scan method.**

Keywords: *pulsed laser deposition, nanostructured thin films, nonlinear optics, z-scan.*

1. Introduction

In recent years, the nonlinear response of nanostructured thin films has been actively discussed due to its dependence on size and shape of nanoparticles contained in films and the ability to control these parameters by changing the coating conditions [1]. Nanostructured metal films have been extensively investigated due to their fast nonlinear response as well as their large nonlinear refractive indices. If a wavelength is close to that of the plasmonic absorption peak of nanoparticles, the nonlinear refractive index of nanostructured metal films increases with increasing local field [2].

Pulsed laser deposition (PLD) is one of the methods used to prepare a variety of nanostructures [3]. The advantages of this method are the ability to control the size of nanoparticles and also to obtain a relatively uniform distribution of nanoparticles on the substrate surface. Among various nanoparticles, copper nanoparticles have attracted much attention due to their fast and high optical nonlinear response.

B. Farmanfarmaei Laser and Optics Research School, P.O. Box 14155-1339, Tehran, Iran; Plasma Physics Research Center, Science and Research Branch, Islamic Azad University, P.O. Box 14665-678, Tehran, Iran;
M.R. RashidianVaziri, F. Hajiesmaeilbaigi Laser and Optics Research School, P.O. Box 14155-1339, Tehran, Iran;
e-mail: rezaeerv@gmail.com

Received 8 September 2013
Kvantovaya Elektronika **44** (11) 1029 – 1032 (2014)
Submitted in English

The effects of their presence in semiconductor thin films, colloids and many different glasses have been studied by Karthikeyan et al. [4].

To measure the nonlinear refractive index, *z*-scan technique can be used which was introduced in 1989 by Sheik-Bahae et al. [5]. This technique for measuring nonlinear refractive indices of thin solid or liquid samples is characterised by high precision in several cases e.g., when fast pulsed lasers are used in experiments [6]. However, in many cases, the *z*-scan theory which is developed for evaluating the nonlinear refractive index is not completely accurate, i.e. when a nonlinear medium exhibits a nonlocal response to laser radiation. For instance, in nematic liquid crystals, reorientation of the director as a result of the optical field action is nonlocal in space. In addition, when a cw or a long-pulse laser is used in *z*-scan experiments and the thermal optical nonlinearity is dominant, the medium response is nonlocal [7]. Recently, a generalised nonlocal *z*-scan theory has been developed for evaluating the second order refractive index of thin samples [8]. In this generalised form, more precise values of the nonlinear refractive index as well as a parameter that determines the nonlocal response of thin samples can easily be found from the measured *z*-scan curves.

In addition to *z*-scan technique, the sign of the nonlinear refractive index of samples can be obtained by observing far-field diffraction rings [9, 10]. Simulations and empirical experiments performed indicate that the sign of the nonlinear refractive index can be determined by analysing the form of the diffraction ring patterns formed in the far-field and by determining the sign of the wave radius of curvature in the entrance plane of the sample [11 – 15]. Simulation of the experiments related to the observation of the diffraction rings in far-field is possible by solving the Fresnel – Kirchhoff integral in the Fraunhofer approximation [10].

In this paper, we describe the preparation of copper nanostructured thin films and measure their nonlinear refractive indices by *z*-scan technique. The diffraction ring patterns after passage of a Gaussian laser beam through the nonlocal nonlinear samples are recorded on a far-field screen. The diffraction patterns obtained are simulated by numerically solving the Fresnel – Kirchhoff integral.

2. Preparation and characterisation of samples

Nanostructured copper thin films were prepared using the PLD method. The second harmonic of an Nd : YAG pulsed laser (wavelength, 532 nm; repetition rate, 10 Hz, and FWHM duration, 20 ns) was used to ablate the copper target inside a vacuum chamber. In order to reduce the detaching possibility of the unwanted macroscopic species from the target surface, its surface was carefully polished with emery papers and thereafter cleaned by ultrasonication in ethanol and deionised water. The laser fluence on the copper surface was ~1.46 J cm^{-2} and a pressure of 200 μTorr was maintained during the deposition process. The laser beam irradiated the copper surface at an angle of 45° with respect to its normal and the target-to-substrate distance was selected equal to 3 cm [16]. The target holder was rotated at 40 rpm to prevent crater formation in a single location on the target surface and the substrate was rotated at 60 rpm to improve the coating layer uniformity. The deposition process continued for 15 min.

After removing the films from the vacuum chamber and before investigating their nonlinear optical properties, optical absorption spectra were measured with a spectrometer in the UV and visible wavelength range. Morphology and mean size of nanoparticles in the prepared nanostructured films were analysed by scanning electron microscopy (SEM).

3. Investigation of the nonlinear refractive index

The *z*-scan technique was used for measuring the nonlinear refractive indices of copper nanostructured thin films. The scheme of the setup used in *z*-scan experiments is shown in Fig. 1. The laser beam is focused by a lens and the sample is moved along the optical axis (the *z* axis) from one to the other side of the focal point. The amount of light passing through a small aperture, which is located far from the focal point, is recorded during the sample movement. Transmission power as a function of the sample location is related to the sign and magnitude of the refractive index, n_2. Our *z*-scan experiments were performed using the second harmonic of a 532-nm, 150-mW cw Nd : YAG laser. The focal length *f* of a lens in the experiment is 25 cm, which leads to a Rayleigh length of 3.4 mm.

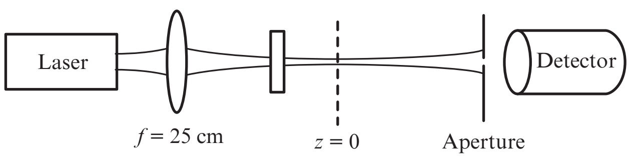

Figure 1. Scheme of the *z*-scan experimental setup.

The nonlocal *z*-scan theory [8] is used for finding the nonlinear refractive indices of copper nanostructured thin films. In the generalised nonlocal *z*-scan theory, the nonlocal parameter *m*, which determines the nonlocal response of the sample, and the second order refractive index n_2 can be obtained from the measured *z*-scan curves. The *m* parameter is calculated from the equation

$$m = \frac{1}{2}\left[\sqrt{\frac{h^2 - 1}{2(7 - h)}} - 1\right], \quad (1)$$

where

$$h = 1 + 6\left(\frac{\Delta z_{\mathrm{p-v}}}{2z_0}\right)^2; \quad (2)$$

z_0 is the Rayleigh length; and $\Delta z_{\mathrm{p-v}}$ is the peak-to-valley separation distance on the measured *z*-scan curve.

By measuring the difference $\Delta T_{\mathrm{p-v}}$ between the peak and valley transmissions in the closed-aperture *z*-scan curve, one can obtain the maximum axial phase shift at the focal point $|\Delta\Phi_0|$ from the equation

$$\Delta T_{\mathrm{p-v}} = \frac{24\sqrt{6}\,(\sqrt{m'} - 1)}{\sqrt{(m' + 7)^2 - 48} + (5m' - 1)} \times \frac{\sqrt{\sqrt{(m' + 7)^2 - 48} - (m' + 1)}}{\sqrt{(m' + 7)^2 - 48} + (5 - m')}\,|\Delta\Phi_0|, \quad (3)$$

where $m' = (2m + 1)^2$. After finding $|\Delta\Phi_0|$, the nonlinear refractive index can be found from the relation

$$n_2 = \frac{\alpha\,|\Delta\Phi_0|}{kI_0[1 - \exp(-\alpha L)]}, \quad (4)$$

where $k = 2\pi/\lambda$ is the wave number; I_0 is the axial intensity at the focal point; α is the linear absorption coefficient; and L is the sample thickness. The sign of the nonlinearity can be determined by locating at the relative position of the peak and the valley on the *z*-scan curve: If a valley is followed by a peak, $n_2 > 0$, and if a peak is followed by a valley, $n_2 < 0$.

To observe the diffraction rings in far-field, a minor change was made in our *z*-scan experimental setup: an aperture and a detector were removed and a CCD camera was placed in the far-field region. The diffraction patterns were projected onto the CCD camera by a lens equipped with a variable aperture diaphragm to avoid the CCD saturation. With this change, diffraction rings can be recorded by camera for any specific *z* positions of the nonlinear sample on the optical axis.

4. Results and discussion

Figure 2 shows a typical absorption spectrum of the films in the UV and visible wavelength range. The presence of plasmonic absorption peaks in the absorption spectra at 619 ± 4 nm is a direct evidence in support of the formation of copper nanoparticles on the film surface [17]. Broadness of the absorption peak in Fig. 2 probably stems from the wide size distribution of copper nanoparticles on the film surface [18].

A typical SEM micrograph of the films is shown in Fig. 3, which confirms the formation of nanoparticles on the surface. One can see that copper nanoparticles have a mean size of 35 ± 11 nm. The large uncertainty in the measured mean size of nanoparticles confirms the wide size distribution of copper nanoparticles on the film surface.

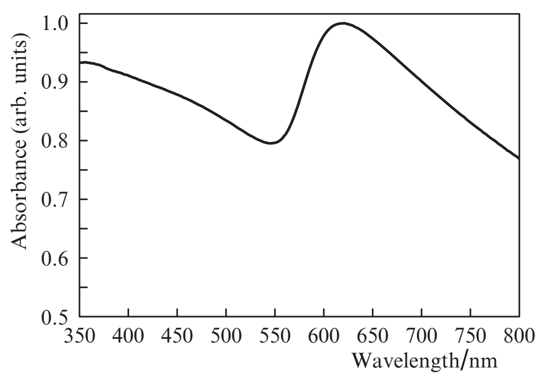

Figure 2. Typical absorption spectrum of copper nanostrutured thin films.

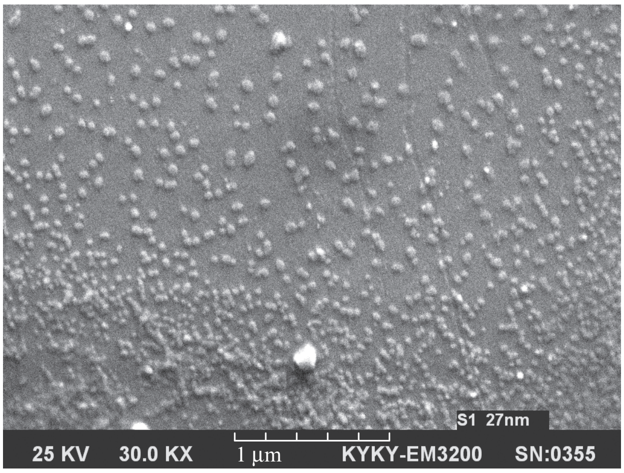

Figure 3. SEM micrograph of the copper nanostructured thin film.

Figure 4 shows a typical closed-aperture *z*-scan curve of nanostructured copper thin films across the optical axis. The nonlocal parameter m is found equal to 2.3 using equations (1) and (2). The obtained m value, which is larger than unity, indicates that the spatial intensity distribution of the diffracted beam is narrower than the beam intensity distribution due to a phase shift in the Gaussian beam impinging on the sample surface [8].

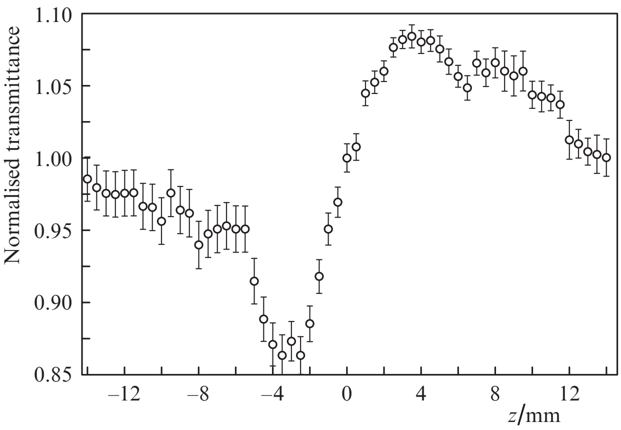

Figure 4. Closed-aperture *z*-scan curve of the copper nanostructured thin film.

The nonlocal response of the copper thin film, whose nanostructure is shown in Fig. 3, can be ascribed to heat diffusion inside the film and scattering of the Gaussian laser beam by nanoparticles. Knowing the value of the m parameter, one can calculate, by using the peak-to-valley transmission difference and equation (3), the maximum nonlinear phase shift, which in our case is equal to 0.7693. Finally, using equation (4), the second order refractive index is determined to be equal to $n_2 = 6\times10^{-6}$ cm^2 W^{-1}, and since in the *z*-scan curve a valley is followed by a peak the refractive index is positive.

Figure 5a shows the recorded diffraction ring pattern on a far-field screen after the laser beam passes through the nonlinear copper thin film. In this case, the sample was located 8 cm behind the focal point. Figure 5b presents the intensity distribution along the radial coordinate. The observed diffraction ring pattern consists of a bright spot in the centre, which conforms to the predictions of Deng et al. [10] that when a divergent Gaussian beam passes through a self-focusing medium ($n_2 > 0$), the obtained ring patterns on a far-field screen should contain a bright spot in the centre. However, we should note that the diffraction rings (Fig. 5a) have low intensity and are completely different from the rings formed during diffraction in nonlinear samples with high values of $|\Delta\Phi_0|$ [10].

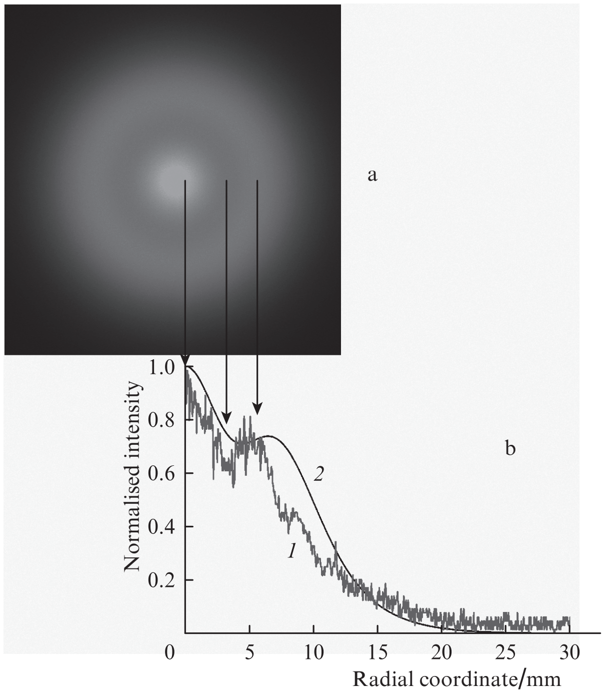

Figure 5. (a) Low-intensity diffraction ring patterns observed on a far-field screen after the beam passage through the sample and (b) intensity distribution along the radial coordinate obtained in the experiment (*1*) and by solving numerically the Fresnel–Kirchhoff diffraction integral.

One should bear in mind that in order to be able to observe diffraction rings arising from the nonlinearity of the sample, the shift $|\Delta\Phi_0|$ should satisfy the condition $|\Delta\Phi_0| \gg 2\pi$ [10]. At the same time, the value of $|\Delta\Phi_0|$ obtained by *z*-scanning of the nanostructured copper thin film was equal to 0.7693. To explain the discrepancy between the predicted and obtained values, one should consider the Fresnel–Kirchhoff diffraction integral in the Fraunhofer approximation which is used for predicting the type of diffraction ring patterns in the far-field

$$I(\rho) = I_0\left|\int_0^\infty J_0(k\theta r)\exp\left[-\frac{r^2}{w^2(z)} - \mathrm{i}\varphi(r)\right]r\mathrm{d}r\right|^2, \qquad (5)$$

where $w(z) = w_0[1 + (z/z_0)^2]^{1/2}$ is the beam radius on the sample at some point z; $J_0(x)$ is the first-kind zero-order Bessel function; θ is the far-field diffraction angle; ρ is the radial coordinate in the far-field observation plane at distance D, which is related to θ as $\rho = D\theta$ in the paraxial approximation; r is the radial coordinate on the sample entrance plane; and $\varphi(r)$ is the total phase shift induced in the Gaussian beam after transmission through the sample, which in the thin sample approximation (i.e., at $L \ll z_0$) [8] can be written as

$$\varphi(r) \approx \frac{kr^2}{2R(z)} + \frac{\Delta\Phi_0}{1+(z/z_0)^2}\exp\left[-\frac{2mr^2}{w^2(z)}\right]. \quad (6)$$

The first term in (6) is related to the natural beam curvature radius $R(z)$ and the second term – to the nonlinear phase shift. By substituting (6) into (5), the first term in the derived equation determines the natural beam diffraction and the second – the diffraction rings arising due to the nonlocal nonlinear Kerr effect.

Figure 5b shows the radial intensity distribution, which is obtained by numerical integration of equation (5) using the parameters corresponding to our experiment. For the nonlocal parameter m and the maximum axial phase shift $|\Delta\Phi_0|$, the values of 2.3 and 0.7693 are respectively used that were obtained using the sample z-scan curve in Fig. 4 and the nonlocal z-scan theory. One can see good agreement between the experimental curve and the curve obtained by solving numerically the Fresnel–Kirchhoff diffraction integral. One should note that the second term in equation (6) is very small. Thus, the observed low-intensity diffraction rings arise due to the presence of the first term in equation (6) that is inversely dependent on the wavefront radius of curvature. As was previously reported [12] the change in $R(z)$ values may also be associated with the formation of diffraction rings. Therefore, the observed low-intensity rings are the result of the natural diffraction of the Gaussian beam and the information contained in these rings cannot be used for evaluating the sign and magnitude of n_2 [9, 12].

5. Conclusions

We have prepared copper nanostructured thin films using the PLD method. For the first time, the nonlocal z-scan theory has been used for obtaining the nonlinear refractive index of copper nanostructured thin films. Because the nanostructure of the material under study determines the nonlocal response and the parameter m, different nanostructures, including those containing nanoparticles, nanorods, nanowires, etc., can be investigated by the proposed method.

It is found that despite the smallness of the maximum axial phase shifts, which were determined using the nonlocal z-scan theory, still some low-intensity ring patterns can be observed on a far-field screen. The stimulation shows that the formation of these rings can be attributed to the variable wavefront curvature radius of the Gaussian beam. Therefore, one must care not to misinterpret these rings as the diffraction rings which can be formed on the far-field screen due to the nonlinear responses of the films.

As we have recently shown [19], in self-phase modulation experiments, which are typically used for evaluating the sign of n_2 [20], the obtained sign may depend on the thickness of the used sample.We believe that the best way for obtaining the sign and magnitude of the nonlinear refractive index of thin samples is the conventional closed-aperture z-scan method.

References

1. Canfield B.K., Kujala S., Jefimovs K., Svirko Y., Turunen J., Kauranen M. *J. Opt. A: Pure Appl. Opt.*, **8**, S278 (2006).
2. Ma G., Sun W., Tang S.H., Zhang H., Shen Z., Qian S. *Opt. Lett.*, **27**, 1043 (2002).
3. Eason R. *Pulsed Laser Deposition of Thin Films: Applications-led Growth of Functional Materials* (New York: John Wiley & Sons Inc., 2007).
4. Karthikeyan B., Anija M., Suchand Sandeep C.S., Muhammad Nadeer T.M., Philip R. *Opt. Commun.*, **281**, 2933 (2008).
5. Sheik-Bahae M., Said A.A., Van Stryland E.W. *Opt. Lett.*, **14**, 955 (1989).
6. Sheik-Bahae M., Said A.A., Wei T.H., Hagan D.J., Van Stryland E.W. *IEEE J. Quantum. Electron.*, **26**, 760 (1990).
7. Dabby F.W., Whinnery J.R. *Appl. Phys. Lett.*, **13**, 284 (1968).
8. Rashidian Vaziri M.R., Hajiesmaeilbaigi F., Maleki M.H. *J. Opt.*, **15** (2), 025201 (2013); Rashidian Vaziri M.R. *Appl. Opt.*, **52**, 4843 (2013).
9. Nascimento C.M., Alencar M.A.R.C., Chávez-Cerda S., da Silva M.G.A., Meneghetti M.R., Hickmann J.M. *J. Opt. A: Pure Appl. Opt.*, **8**, 947 (2006).
10. Deng L., He K., Zhou T., Li C. *J. Opt. A: Pure Appl. Opt.*, **7**, 409 (2005).
11. Karimzadeh R. *Opt. Commun.*, **286**, 329 (2013).
12. Ramirez E.V.G., Carrasco M.L.A., Otero M.M.M., Cerda S.C., Castillo M.D.I. *Opt. Express*, **18**, 22067 (2010).
13. Yokota Y., Ogusu K., Tanaka Y. *IEICE Trans. Electron. E*, **81-C**, 455 (1998).
14. Durbin S.D., Arakelian S.M., Shen Y.R. *Opt. Lett.*, **6**, 411 (1981).
15. Koushki E., Farzaneh A., Mousavi S.H. *J. Phys. B: Appl. Phys.*, **99**, 565 (2010).
16. Rashidian Vaziri M.R., Hajiesmaeilbaigi F., Maleki M.H. *J. Phys. D: Appl. Phys.*, **43**, 425205 (2010).
17. Magruder R.H., Haglund R.F., Yang L., Witting J.E., Zuhr R.A. *J. Appl. Phys.*, **76**, 708 (1994).
18. Arul Dhas N., Paul Raj C., Gedanken A. *Chem. Mater.*, **10**, 1446 (1998).
19. Rashidian Vaziri M.R., Hajiesmaeilbaigi F., Maleki M.H. *J. Opt.*, **15** (3), 035202 (2013).
20. Lucchetti L., Suchand S., Simoni F. *J. Opt. A: Pure Appl. Opt.*, **11**, 034002 (2009).